

Intramolecular Nonbonded S···N Interaction in Rabeprazole

Kazuhiko HAYASHI,^{*,a} Shiho OGAWA,^b Shigeki SANO,^b Motoo SHIRO,^c Kentaro YAMAGUCHI,^d Yoshihisa SEI,^d and Yoshimitsu NAGAO^{*,b}

^a College of Pharmacy, Kinjo Gakuin University; 2-1723 Omori, Moriyama-ku, Nagoya 463-8521, Japan; ^b Graduate School of Pharmaceutical Sciences, The University of Tokushima; Sho-machi, Tokushima 770-8505, Japan; ^c Rigaku Corporation; 3-9-12 Matsubara-cho, Akishima, Tokyo 196-8666, Japan; and ^d Faculty of Pharmaceutical Sciences at Kagawa Campus, Tokushima Bunri University; 1314-1 Shido, Sanuki, Kagawa 769-2193, Japan.

Received January 8, 2008; accepted March 21, 2008; published online April 1, 2008

Intramolecular nonbonded S···N interactions in the crystal structures of the derivatives (7a–d) of sodium rabeprazole (1) and an intermolecular nonbonded S···N interaction between ethylmethylsulfoxide and pyridine in a solution were recognized. These results made us estimate that the intramolecular nonbonded S···N interaction existed in 1 and its derivatives in a solution, and formed the 4-membered quasi-ring in 2 (Fig. 1) followed by the increase of the reactivity of 2 to give the putative spiro sulfoxide 3, which is the key intermediate in the reaction cascade of 1 (Chart 1).

Key words nonbonded interaction; rabeprazole; X-ray crystallographic analysis; proton pump inhibitor; close contact

Intramolecular nonbonded S···X (X=S, O, N, etc.) interactions have been observed in a large number of organosulfur compounds controlling the conformation of small and large molecules.^{1–12} Some of these compounds showed the strong bioactivity, and we suggested that the intramolecular nonbonded S···X interactions play an important role on the mechanism of several biological effects.^{1,2,6–12} For example, the clear S···O close contact in the complex crystalline structure of carbonic anhydrase I and acetazolamide was recognized.¹² The same nonbonded interaction was observed in the crystalline structure of acyliminothiadiazoline, which has potent angiotensin II receptor antagonistic activity.^{6,11} It is estimated that the ring structure consisted of the intramolecular nonbonded S···X interactions was more flexible than that of covalent bonding, and this flexibility increased the binding affinity of the active compound to the flexible pocket of the enzyme or the receptor. These results prompted us to disclose the new roles of intramolecular nonbonded S···X interactions in other drugs. Herein, we focus on rabeprazole, ^{13–16} and discuss the intramolecular nonbonded S···N interaction in rabeprazole and its role.

Sodium rabeprazole (**1**) is one of the inhibitors of the gastric (H⁺-K⁺)-ATPase.^{13,14} As a result of the investigations on the mechanism of action of these inhibitors, it has been expected that **1** will be activated by protonation in the parietal cell (intermediate **2**), converted into the sulfenamide **5** via the spiro sulfoxide **3** and sulfenic acid **4**, and the active principle **5** can react with the accessible cysteines of the gastric (H⁺-K⁺)-ATPase followed by the inhibition of the enzyme (compound **6**), as shown in Chart 1.^{14,17–20} In this reaction cascade, the key step is the formation of the putative spiro sulfoxide **3** arising from nucleophilic attack of the pyridine nitrogen on the activated 2-position of the benzimidazole moiety.¹⁸ The fact that the nucleophilic attack of the pyridine nitrogen smoothly proceeds despite the weak nucleophilicity is very interest, and made us guess that the intramolecular nonbonded S···N interaction influenced this step. Because, if such intramolecular nonbonded S···N interaction is possible in rabeprazole, the 4-membered quasi-ring in **2** containing the rabeprazole structure would be formed and bring the nitrogen atom of pyridine close to the

electrophilic position of benzimidazole moiety, as shown in Fig. 1. Therefore, in order to make clear the presence of the intramolecular nonbonded S···N interaction in **1**, we characterized the crystal structures of derivatives of **1** at first, since **1** itself could hardly be crystallized.²¹

The reactions of **1** with various electrophiles in the presence of amines gave the corresponding derivatives of **1** in 36–92% yields, as shown in Chart 2. The resultant derivatives **7a–d** were recrystallized from suitable solvents to obtain the corresponding crystals available for X-ray crystallographic analysis. The computer-generated drawings of the crystal structures of derivatives **7a–d** are shown in Fig. 2. As we expected, the S···N close contact between sulfoxide S and N of the pyridine moiety was recognized in crystal structures of all derivatives. In crystallographic structures **7a–c**, the distances (2.815, 2.806, 2.709 Å) between nonbonded S···N atoms were clearly shorter than the sum (S and N:

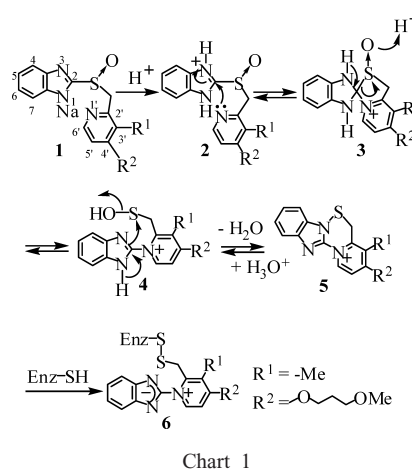


Chart 1

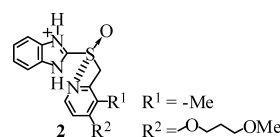


Fig. 1. Probable Nonbonded S···N Interaction in **2**

* To whom correspondence should be addressed. e-mail: hayashi@kinjo-u.ac.jp

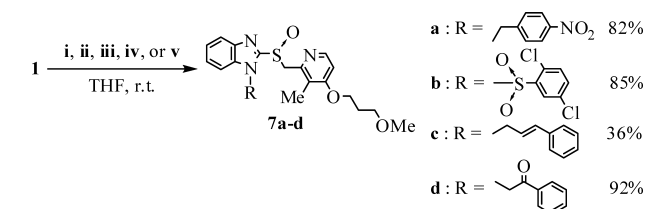
3.35 Å)²²⁾ of the corresponding van der Waals radii, and the planarities of S–C–C–N (see torsion angles in **7a–c**) moieties were determined. And, the S···N close contact (S1···N3: 3.229 Å, 3.235 Å) can also be observed in the crystallographic structure of **7d**, though the planarity of the S1–C16–C17–N3 moiety was not recognized. These results make us estimate that the S···N close contact is formed in the crystal structure of **1**, and get us interested in this S···N close contact in a solution. In previous studies, we have reported the evidence for intermolecular nonbonded S···O interactions in a solution by utilizing cold-spray ionization mass spectrometry (CSI-MS).²³⁾ Thus, we attempted detection of a weak complex of ethylmethylsulfoxide with pyridine by an intermolecular nonbonded S···N interaction in a MeOH solution in a similar manner, since a nonbonded S···N interaction has not been detected in a solution.

The CSI-MS spectra were taken by using mixture (1 : 1) of ethylmethylsulfoxide with an equimolar amount of pyridine in MeOH at room temperature, and the corresponding molecular ion peak, *m/z* 172 due to [ethylmethylsulfoxide···pyridine complex+H]⁺ (for C₈H₁₃NOS+H), were clearly observed, as shown in Fig. 3. This result suggests that

a nonbonded S···N interaction was formed between ethylmethylsulfoxide molecule and pyridine molecule in a MeOH solution and the same nonbonded S···N interaction can also be formed within a molecule. Therefore, we estimate that the intramolecular nonbonded S···N interaction is formed in **1** itself even in a solution, and the 4-membered quasi-ring formed by the nonbonded interaction in **2** containing the rabeplazole structure accelerates the reaction of **2** to **3**.

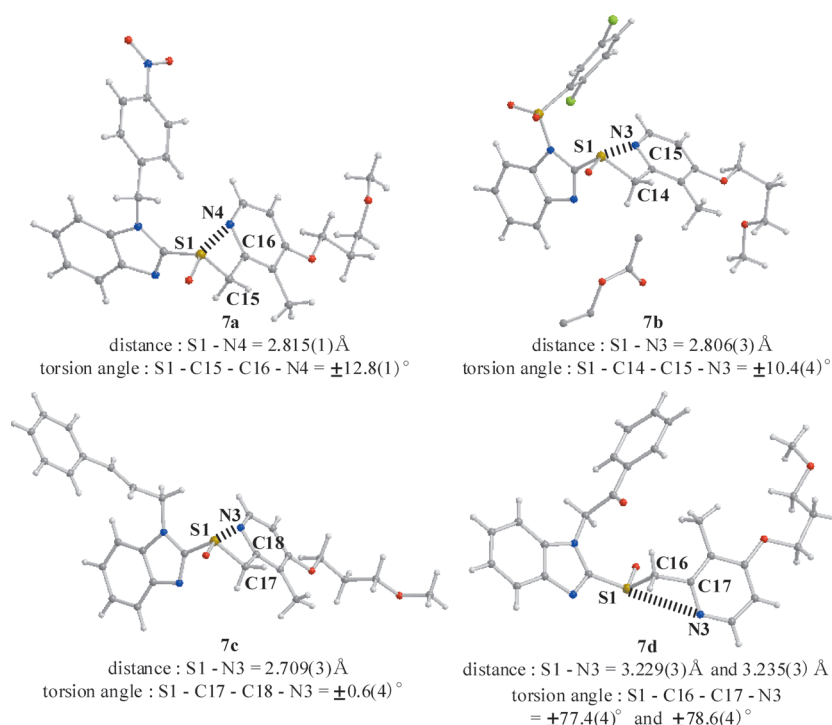
Subsequently, the intermediates, which were formed in the reaction cascade^{17–20)} to inhibit the gastric (H⁺-K⁺)-ATPase, were isolated in order to make clear that the action mechanism of **1** was the same as that of the other inhibitors of the gastric (H⁺-K⁺)-ATPase. The sulfenamide **8e** was obtained in 86% yield by the treatment of **1** with 48% aqueous HBF₄ in methanolic solution.¹⁸⁾ Using 60% HClO₄, the perchlorate salt **8f** was obtained in a quantitative yield, as shown in Chart 3. The reaction of **8e** with ethanethiol gave the desired disulfide **9** in 99% yield, as shown in Chart 4. The structures of these compounds were identified by ¹H-NMR, IR spectra, mass spectra, and elementary analysis. Interestingly, the reaction of **8e** with cysteine afforded cystine in 72% yield, as shown in Chart 4. In preceding paper, it has been reported that the S–S bond in **9** can be cleaved by thiols yielding another disulfides.¹⁷⁾ In this reaction, the rate of nucleophilic attack of cysteine to disulfide **10**, which should be generated by the reaction of **8e** with cysteine, would be much faster than that to **8e**, as shown in Fig. 4. The generation of **8e**, **8f**, **9**, and cystine definitely suggest that sodium rabeplazole (**1**) also inhibits the gastric (H⁺-K⁺)-ATPase in the action mechanism reported previously,^{18–20)} and the same intramolecular nonbonded S···N interactions will also exist in the other inhibitors of the gastric (H⁺-K⁺)-ATPase such as lansoprazole²⁴⁾ and omeprazole.²⁵⁾

In conclusion, the intramolecular nonbonded S···N interactions in the crystal structures of rabeplazole derivatives



Reagents and conditions: (i) 4-nitrobenzylbromide (1.2 mol eq), *N,N*-diisopropylethylamine (2.2 mol eq), 18 h; (ii) 2,5-dichlorobenzoyl chloride (1.1 mol eq), Et₃N (3.0 mol eq), 13 h; (iii) cinnamyl bromide (1.2 mol eq), Et₃N (2.2 mol eq), 20.5 h; (iv) 2-bromoacetophenone (1.1 mol eq), Et₃N (3.0 mol eq), 17.5 h.

Chart 2

Fig. 2. Computer-Generated Drawing Derived from the X-Ray Coordinates of Compounds **7a–d**

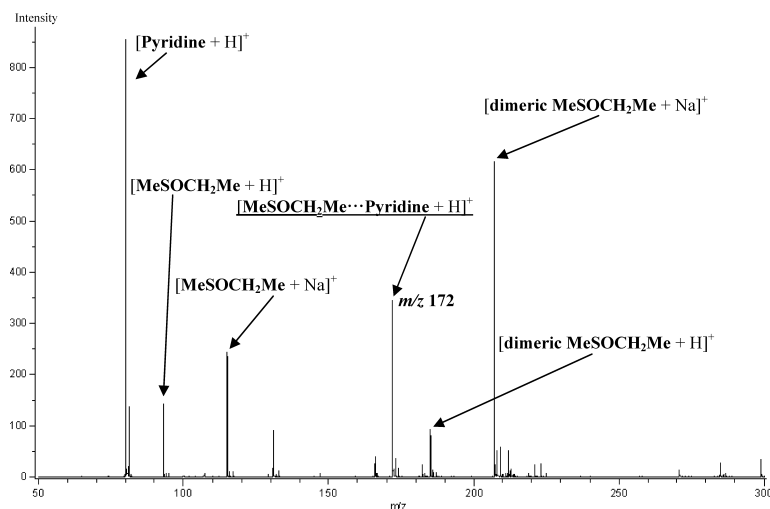
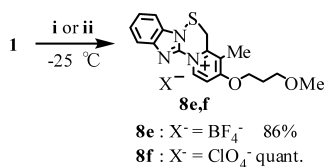
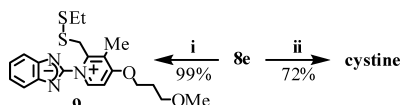


Fig. 3. CSI Mass Spectrum of Ethylmethylsulfoxide and Pyridine



Reagents and conditions: (i) aq. HBF_4 (3.3 mol eq), MeOH, 14 h; (ii) aq. HClO_4 (3.3 mol eq), MeOH, 16 h.

Chart 3



Reagents and conditions: (i) EtSH (1.0 mol eq), MeCN, 1 N HCl (cat.), r.t., 1.5 h; (ii) cysteine (1.0 mol eq), 50% aq. MeCN, 1 N HCl (cat.), r.t., 17 h.

Chart 4

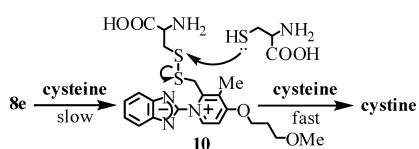


Fig. 4. Plausible Cystine-Generating Pathway from **8e**

7a—d and the intermolecular nonbonded $\text{S}\cdots\text{N}$ interaction between ethylmethylsulfoxide S and N of the pyridine moiety in a solution were recognized. From these results, it is assumed that the nonbonded $\text{S}\cdots\text{N}$ interaction in **1** is formed in a solution, and increase the reactivity of **2** to give the putative spiro sulfoxide **3** by the formation of the 4-membered quasi-ring in **2** containing the rabeprazole structure, as shown in Chart 1 and Fig. 1. Further, the mechanism of action of sodium rabeprazole (**1**) was confirmed by the isolation of the intermediates (**8e**, **8f**, **9**, and cystine) in the reaction cascade of **1**.

Experimental

All melting points were determined on a Yanaco micro melting point apparatus and are uncorrected. IR spectra were obtained on a JASCO FT/IR-420 IR Fourier transform spectrometer. $^1\text{H-NMR}$ (400 MHz) spectra were recorded on JEOL JNM-AL400. Chemical shifts are given in δ values (ppm)

using tetramethylsilane (TMS) as an internal standard. Fast atom bombardment mass spectra (FAB-MS) were recorded on a JEOL JMS SX-102A spectrometer. Cold-spray ionization mass spectra (CSI-MS) were measured by JEOL JMS-700 spectrometer equipped with CSI source. Elementary combustion analyses were performed on a Yanaco CHN CORDER MT-5. All reactions were monitored by TLC employing 0.25-mm silica gel plates (Merck 5715; 60 F_{254}). Column chromatography was carried out on silica gel [Kanto Chemical 60N; 63—210 μm]. Anhydrous THF was commercially obtained from Kanto Chemical. All reagents were used as purchased.

Typical Procedure for the Preparation of Rabeprazole Derivatives 7a—d 4-Nitrobenzylbromide (1.36 g, 6.30 mmol) was added to a solution of *N,N*-diisopropylethylamine (2.00 ml, 11.5 mmol) and **1** (2.00 g, 5.24 mmol) in anhydrous THF (2.0 ml) at -26°C . After being stirred at room temperature for 18 h, the reaction mixture was treated with water and then extracted with CHCl_3 . The extract was washed with saturated NaHCO_3 solution, saturated NH_4Cl solution, and brine, and then dried over anhydrous MgSO_4 . The organic layer was evaporated *in vacuo* to afford a crude product, which was purified by chromatography on a silica gel column [CHCl_3 and $\text{CHCl}_3/\text{MeOH}$ (97 : 3)], giving **7a** (2.13 g, 82%) as colorless powder. The single crystals of **7a** were obtained by recrystallization from THF as colorless prisms.

1-(4-Nitrobenzyl)-2- $\{[4-(3\text{-methoxypropoxy})\text{-3-methylpyridin-2-yl]methylsulfinyl}\}$ -1*H*-benzimidazole (**7a**): Colorless prisms, mp 143°C (THF). $^1\text{H-NMR}$ (400 MHz, CDCl_3) δ : 2.0—2.1 (2H, m), 2.23 (3H, s), 3.35 (3H, s), 3.55 (2H, t, $J=6.1$ Hz), 4.08 (2H, t, $J=6.1$ Hz), 4.99 (1H, d, $J=13.7$ Hz), 5.12 (1H, d, $J=13.7$ Hz), 5.79 (1H, d, $J=16.4$ Hz), 5.86 (1H, d, $J=16.4$ Hz), 6.66 (1H, d, $J=5.6$ Hz), 7.23 (1H, d, $J=7.6$ Hz), 7.3—7.4 (4H, m), 7.86 (1H, d, $J=7.6$ Hz), 8.10 (1H, d, $J=5.6$ Hz), 8.16 (2H, d, $J=8.6$ Hz). IR (KBr) cm^{-1} : 2875, 1585, 1521, 1341, 1341, 1038, 744, 429. FAB-MS m/z : 495.1700 [$\text{M}+1$] $^+$ (Calcd for $\text{C}_{25}\text{H}_{27}\text{N}_4\text{O}_5\text{S}$: 495.1702). *Anal.* Calcd for $\text{C}_{25}\text{H}_{26}\text{N}_4\text{O}_5\text{S}$: C, 60.71; H, 5.30; N, 11.33. Found: C, 60.47; H, 5.28; N, 11.04.

1-(2,4-Dichlorophenylsulfonyl)-2- $\{[4-(3\text{-methoxypropoxy})\text{-3-methylpyridin-2-yl]methylsulfinyl}\}$ -1*H*-benzimidazole (**7b**): Colorless needles, mp $124\text{—}125^\circ\text{C}$ (AcOEt). $^1\text{H-NMR}$ (400 MHz, CDCl_3) δ : 2.0—2.1 (2H, m), 2.26 (3H, s), 3.36 (3H, s), 3.55 (2H, t, $J=6.1$ Hz), 4.08 (2H, t, $J=6.1$ Hz), 4.78 (1H, d, $J=13.4$ Hz), 4.96 (1H, d, $J=13.4$ Hz), 6.63 (1H, d, $J=5.6$ Hz), 7.4—7.5 (3H, m), 7.56 (1H, dd, $J=2.4, 8.3$ Hz), 7.7—7.8 (1H, m), 7.8—7.9 (1H, m), 8.10 (1H, d, $J=5.6$ Hz), 8.41 (1H, d, $J=2.4$ Hz). IR (KBr) cm^{-1} : 1583, 1454, 1387, 1296, 1171, 1055, 823, 688, 584, 523. FAB-MS m/z : 568.0530 [$\text{M}+1$] $^+$ (Calcd for $\text{C}_{24}\text{H}_{24}\text{Cl}_2\text{N}_3\text{O}_5\text{S}_2$: 568.0534). *Anal.* Calcd for $\text{C}_{24}\text{H}_{23}\text{Cl}_2\text{N}_3\text{O}_5\text{S}_2 \cdot 1/4\text{AcOEt}$: C, 50.85; H, 4.27; N, 7.12. Found: C, 50.62; H, 4.18; N, 6.95.

1-Cinnamyl-2- $\{[4-(3\text{-methoxypropoxy})\text{-3-methylpyridin-2-yl]methylsulfinyl}\}$ -1*H*-benzimidazole (**7c**): Colorless plates, mp $97\text{—}98^\circ\text{C}$ (Et_2O). $^1\text{H-NMR}$ (400 MHz, CDCl_3) δ : 2.0—2.1 (2H, m), 2.22 (3H, s), 3.34 (3H, s), 3.53 (2H, t, $J=6.1$ Hz), 4.04 (2H, t, $J=6.1$ Hz), 4.97 (1H, d, $J=13.6$ Hz), 5.04 (1H, d, $J=13.6$ Hz), 5.25 (1H, ddd, $J=1.2, 5.9, 16.4$ Hz), 5.30 (1H, ddd, $J=1.2, 5.9, 16.4$ Hz), 6.32 (1H, dt, $J=15.9, 5.9$ Hz), 6.59 (1H, d, $J=15.9$ Hz), 6.63 (1H, d, $J=5.9$ Hz), 7.2—7.4 (7H, m), 7.4—7.5 (1H, m), 7.8—7.9 (1H, m), 8.17 (1H, d, $J=5.6$ Hz). IR (KBr) cm^{-1} : 2939, 1581,

Table 1. Summary of X-Ray Crystallographic Analyses of Compounds **7a**—**d**

	7a	7b	7c	7d
Formula	C ₂₅ H ₂₆ N ₄ O ₅ S	C ₂₆ H ₂₇ Cl ₂ N ₃ O ₆ S ₂	C ₂₇ H ₂₉ N ₃ O ₃ S	C ₂₆ H ₂₇ N ₃ O ₄ S
Formula weight	494.56	612.54	475.60	477.58
Crystal description	Colorless, block	Colorless, platelet	Colorless, platelet	Colorless, block
Crystal system	Monoclinic	Triclinic	Monoclinic	Triclinic
Space group	<i>P</i> 2 ₁ / <i>c</i>	<i>P</i> $\bar{1}$	<i>P</i> 2 ₁ / <i>c</i>	<i>P</i> $\bar{1}$
Lattice constants				
<i>a</i> , Å	10.063(5)	7.880(11)	12.216(8)	8.451(4)
<i>b</i> , Å	8.448(4)	12.902(16)	8.772(5)	15.885(7)
<i>c</i> , Å	27.950(1)	14.304(17)	23.000(18)	17.750(8)
α , deg.		96.63(8)		89.54(3)
β , deg.	94.82(2)	103.56(8)	90.16(5)	86.08(3)
γ , deg.		96.05(9)		85.90(3)
Volume, Å ³	2366(1)	1391(3)	2465(3)	2371(18)
Z	4	2	4	4
Density (calcd), g/cm ³	1.388	1.462	1.282	1.338
Residual <i>R</i> , <i>R</i> _w	0.043, 0.083	0.069, 0.182	0.134, 0.187	0.098, 0.247
Goodness of Fit Indicator	1.065	1.146	0.917	1.203

1458, 1296, 1088, 1041, 756. FAB-MS *m/z*: 476.1982 [M+1]⁺ (Calcd for C₂₇H₃₀N₃O₃S: 476.2008). *Anal.* Calcd for C₂₇H₂₉N₃O₃S: C, 68.18; H, 6.15; N, 8.84. Found: C, 68.21; H, 6.19; N, 8.71.

1-Phenacyl-2-[[4-(3-methoxypropoxy)-3-methylpyridin-2-yl]methylsulfanyl]-1*H*-benzimidazole (**7d**): Colorless needles, mp 108–109 °C (AcOEt). ¹H-NMR (400 MHz, CDCl₃) δ : 2.0–2.1 (2H, m), 2.16 (3H, s), 3.34 (3H, s), 3.53 (2H, t, *J*=6.1 Hz), 4.07 (2H, t, *J*=6.1 Hz), 4.87 (1H, d, *J*=13.9 Hz), 4.95 (1H, d, *J*=13.9 Hz), 5.94 (1H, d, *J*=18.3 Hz), 6.21 (1H, d, *J*=18.3 Hz), 6.68 (1H, d, *J*=5.6 Hz), 7.2–7.3 (1H, m), 7.3–7.4 (2H, m), 7.54 (2H, t, *J*=7.3 Hz), 7.67 (1H, t, *J*=7.3 Hz), 7.8–7.9 (1H, m), 8.04 (2H, d, *J*=7.3 Hz), 8.23 (1H, d, *J*=5.6 Hz). IR (KBr) cm⁻¹: 2939, 2877, 1689, 1581, 1458, 1234, 1088, 748. FAB-MS *m/z*: 478.1790 [M+1]⁺ (Calcd for C₂₆H₂₈N₃O₄S: 478.1807). *Anal.* Calcd for C₂₆H₂₇N₃O₄S: C, 65.39; H, 5.70; N, 8.80. Found: C, 65.19; H, 5.70; N, 8.78.

X-Ray Crystallographic Analysis of Rabepazole Derivatives **7a**—**d**

The measurement was made on a Rigaku RAXIS-RAPID Imaging Plate diffractometer with graphite monochromated MoK α radiation. The data were processed using the PROCESS-AUTO program package. The linear absorption coefficient, μ , for MoK α radiation is 1.0 cm⁻¹. A symmetry-related absorption correction using the program ABCOR was applied.²⁶⁾ The data were corrected for Lorentz and polarization effects. The structure was solved by directed methods and expanded using Fourier techniques.^{27,28)} The non-hydrogen atoms were refined anisotropically. Hydrogen atoms were included but not refined. Natural atom scattering factors were taken from Cromer and Waber.²⁹⁾ The values for the mass attenuation coefficients are those of Creagh and Hubbel.³⁰⁾ All calculation were performed using the teXsan crystallographic software package.³¹⁾ The crystal data are listed in Table 1.

Determination Condition for CSI-MS (Cold-Spray Ionization Mass Spectrometry)²³⁾ Needle voltage: 3.9 kV, orifice voltage: 30 V, ring lens voltage: 10 V, spray temp.: r.t., resolution: 6000, flow rate: 0.5 ml/h, solvent: MeOH, CSI mass spectra of ethylmethylsulfoxide and pyridine: [C₈H₁₃NOS+H]⁺, exact mass: 172.0649.

Typical Procedure for the Preparation of Sulfenamide **8e, **f**** 48% aqueous HBF₄ (1.4 ml, 10.7 mmol) was added to a solution of **1** (2.00 g, 5.24 mmol) in MeOH (60 ml) at -25 °C. After being stirred for 14 h, the precipitated yellow powder was collected by filtration, washed with cold MeOH and then dried *in vacuo* to give **8e** (1.92 g, 86%).

3-(3-Methoxypropoxy)-4-methyl-5*H*-pirido[1'.2':4.5][1.2.4]thiadiazino[2.3-*a*]benzimidazol-13-ium Tetrafluoroborate (**8e**): Yellow powder, mp 123 °C (dec.). ¹H-NMR (400 MHz, DMSO-*d*₆) δ : 2.0–2.2 (2H, m), 2.42 (3H, s), 3.29 (3H, s), 3.55 (2H, t, *J*=6.1 Hz), 4.62 (2H, t, *J*=6.4 Hz), 5.11 (2H, s), 7.3–7.5 (2H, m), 7.70 (1H, d, *J*=7.8 Hz), 7.86 (1H, d, *J*=7.8 Hz), 7.89 (1H, d, *J*=7.8 Hz), 9.56 (1H, d, *J*=7.8 Hz). IR (KBr) cm⁻¹: 3433, 1624, 1450, 1315, 1084, 756. FAB-MS *m/z*: 342.1293 [M]⁺ (Calcd for C₁₈H₂₀N₃O₂S: 342.1276). *Anal.* Calcd for C₁₈H₂₀N₃O₂S·BF₄·CH₃OH: C, 49.80; H, 4.62; N, 9.17. Found: C, 49.54; H, 4.64; N, 9.54.

3-(3-Methoxypropoxy)-4-methyl-5*H*-pirido[1'.2':4.5][1.2.4]thiadiazino[2.3-*a*]benzimidazol-13-ium Perchlorate (**8f**): Colorless powder, mp 123 °C (dec.). ¹H-NMR (400 MHz, DMSO-*d*₆) δ : 2.1–2.2 (2H, m), 2.42 (3H, s), 3.28 (3H, s), 3.55 (2H, t, *J*=6.1 Hz), 4.62 (2H, t, *J*=6.1 Hz), 5.10 (2H, s), 7.4–7.5 (2H, m), 7.70 (1H, d, *J*=7.6 Hz), 7.86 (1H, d, *J*=8.1 Hz),

7.89 (1H, d, *J*=7.6 Hz), 9.55 (1H, d, *J*=7.6 Hz). IR (KBr) cm⁻¹: 1621, 1564, 1520, 1475, 1415, 1317, 1101, 1068, 762, 623. FAB-MS *m/z*: 342.1251 [M]⁺ (Calcd for C₁₈H₂₀N₃O₂S: 342.1276). *Anal.* Calcd for C₁₈H₂₀N₃O₂S·ClO₄·1/2CH₃OH: C, 48.53; H, 4.84; N, 9.18. Found: C, 48.21; H, 4.54; N, 9.52.

Reaction of **8e with Ethanthiol** 1 N HCl (0.2 ml) and ethanthiol (35 ml, 0.94 mmol) were added to a solution of **8e** (400 mg, 0.94 mmol) in MeCN (4 ml) at room temperature. After being stirred at room temperature for 30 min, the reaction mixture was treated with saturated NaHCO₃ solution, concentrated *in vacuo*, and then extracted with AcOEt. The extract was dried over anhydrous MgSO₄ and evaporated *in vacuo* to afford a residue, which was crystallized from AcOEt to give **9** (381 mg, 99%).

2-[2-(Ethylidithiomethyl)-4-(3-methoxypropoxy)-3-methyl-1-pyridinio]benzimidazolide (**9**): Yellow powder, mp 92 °C. ¹H-NMR (400 MHz, CDCl₃) δ : 1.02 (3H, t, *J*=7.3 Hz), 2.2–2.3 (2H, m), 2.31 (2H, q, *J*=7.3 Hz), 2.48 (3H, s), 3.39 (3H, s), 3.59 (2H, t, *J*=6.4 Hz), 4.42 (2H, t, *J*=6.4 Hz), 4.89 (2H, s), 7.12 (1H, d, *J*=7.3 Hz), 7.1–7.2 (2H, m), 7.7–7.8 (2H, m), 8.96 (1H, d, *J*=7.1 Hz). IR (KBr) cm⁻¹: 2880, 1619, 1307, 1091, 750; FAB-MS *m/z*: 404.1473 [M]⁺ (Calcd for C₂₀H₂₅N₃O₂S₂: 404.1466). *Anal.* Calcd for C₂₀H₂₅N₃O₂S₂·1/4H₂O: C, 58.09; H, 6.46; N, 10.16. Found: C, 58.36; H, 6.13; N, 10.10.

Reaction of **8e with Cysteine**³²⁾ 1 N HCl (0.25 ml) and a solution of L-cysteine (142 mg, 1.17 mmol) in water (2.5 ml) were added to a solution of **8e** (500 mg, 1.17 mmol) in MeCN (2.5 ml) at room temperature. After being stirred at room temperature for 16.5 h, the precipitated colorless powder was collected by filtration, washed with water, and then dried *in vacuo* to give cysteine (101 mg, 72%).

Cystine: Colorless powder, 258–261 °C (dec.) [lit.³³⁾ 260–261 °C (dec.)]. ¹H-NMR (400 MHz, D₂O+NaOD) δ : 2.90 (2H, dd, *J*=7.6, 13.7 Hz), 3.10 (2H, dd, *J*=4.6, 13.7 Hz), 3.58 (2H, dd, *J*=4.6, 7.6 Hz); IR (KBr) cm⁻¹: 1585, 1484, 1408, 1194, 1127, 963, 847, 541.

Acknowledgement We thank Eisai Co., Ltd., for the provision of sodium rabepazole (**1**). This work was supported by a Grant-in-Aid for Scientific Research (B) (2) (14370723 and 16390008) and Scientific Research (C) (20550102) from the Japan Society for the Promotion of Science.

References and Notes

- Burling T. F., Goldstein B. M., *J. Am. Chem. Soc.*, **114**, 2313–2320 (1992).
- Tanaka R., Oyama Y., Imajo S., Matsuki S., Ishiguro M., *Bioorg. Med. Chem.*, **5**, 1389–1399 (1997).
- Hansen L. K., Hordvik A., Saethre L. J., "Organic Sulfur Chemistry," ed. by Stirling C. J. M., Butterworths, London, 1975, pp. 1–17.
- Kucsman A., Kapovits I., "Organic Sulfur Chemistry, Theoretical and Experimental Advances," ed. by Bernardi F., Csizmadia I. G., Mangini A., Elsevier, Amsterdam, 1985, pp. 191–245.
- Ohkata K., Ohsugi M., Yamamoto K., Ohsawa M., Akiba K., *J. Am. Chem. Soc.*, **118**, 6355–6369 (1996).
- Nagao Y., Hirata T., Goto S., Sano S., Kakehi A., Iizuka K., Shiro M., *J. Am. Chem. Soc.*, **120**, 3104–3110 (1998).

- 7) Kumagai T., Tamai S., Abe T., Matsunaga H., Hayashi K., Kishi I., Shiro M., Nagao Y., *J. Org. Chem.*, **63**, 8145—8149 (1998).
- 8) Nagao Y., Nishijima H., Iimori H., Ushiroguchi H., Sano S., Shiro M., *J. Organomet. Chem.*, **611**, 172—177 (2000).
- 9) Nagao Y., Iimori H., Nam K. H., Sano S., Shiro M., *Chem. Pharm. Bull.*, **49**, 1660—1661 (2001).
- 10) Nagao Y., Miyamoto S., Hayashi K., Mihira A., Sano S., *Chem. Pharm. Bull.*, **50**, 558—562 (2002).
- 11) Nagao Y., Iimori H., Goto S., Hirata T., Sano S., Chuman H., Shiro M., *Tetrahedron Lett.*, **43**, 1709—1712 (2002).
- 12) Nagao Y., Honjo T., Iimori H., Goto S., Sano S., Shiro M., Yamaguchi K., Sei Y., *Tetrahedron Lett.*, **45**, 8757—8761 (2004).
- 13) Morii M., Takata H., Fujisaki H., Takeguchi N., *Biochem. Pharmacol.*, **39**, 661—667 (1990).
- 14) Fujisaki H., Oketani K., Shibata H., Murakami M., Fujimoto M., Wakabayashi T., Yamatsu I., Takeguchi N., *Nippon Yakurigaku Zasshi*, **102**, 389—397 (1993).
- 15) Mori M., Hamatani K., Takeguchi N., *Biochem. Pharmacol.*, **49**, 1729—1734 (1995).
- 16) Yasuda S., Ohnishi A., Ogawa T., Tomono Y., Hasegawa J., Nakai H., Shimamura Y., Morishita N., *Int. J. Pharmacol. Ther.*, **32**, 466—473 (1994).
- 17) Figala V., Klemm K., Kohl B., Kruger U., Rainer G., Schaefer H., Senn-Bilfinger J., Sturm E., *J. Chem. Soc. Chem. Commun.*, **1986**, 125—127 (1986).
- 18) Senn-Bilfinger J., Kruger U., Sturm E., Figala V., Klemm K., Kohl B., Rainer G., Schaefer H., Blake T. J., Darkin D. W., Ife R. J., Leach C. A., Mitchell R. C., Pepper E. S., Salter C. J., Viney N. J., Huttner G., Zsolnai L., *J. Org. Chem.*, **52**, 4582—4592 (1987).
- 19) Kruger U., Senn-Bilfinger J., Sturm E., Figala V., Klemm K., Kohl B., Rainer G., Schaefer H., Blake T. J., Darkin D. W., Ife R. J., Leach C. A., Mitchell R. C., Pepper E. S., Salter C. J., Viney N. J., *J. Org. Chem.*, **55**, 4163—4168 (1990).
- 20) Shin J. M., Cho Y. M., Sachs G., *J. Am. Chem. Soc.*, **126**, 7800—7811 (2004).
- 21) Nochi S., Kawai T., Kawakami Y., Asakawa N., Ueda N., Hayashi K., Souda S., *Chem. Pharm. Bull.*, **44**, 1853—1857 (1996).
- 22) Bondi A., *J. Phys. Chem.*, **68**, 441—451 (1964).
- 23) Nagao Y., Miyamoto S., Miyamoto M., Takeshige H., Hayashi K., Sano S., Shiro M., Yamaguchi K., Sei Y., *J. Am. Chem. Soc.*, **128**, 9722—9729 (2006).
- 24) Barradell L. B., Faulds D., McTavish D., *Drugs*, **44**, 225—250 (1992).
- 25) Clissold S. P., Campoli-Richards D. M., *Drugs*, **32**, 15—47 (1986).
- 26) ABCOR: Higashi T., 1995. Program for Absorption Correction, Rigaku Corporation, Tokyo, Japan.
- 27) SIR97: Altomare A., Burla M. C., Camalli M., Cascarano G. L., Giacovazzo C., Guagliardi A., Moliterni A. G. G., Polidori G., Spagna R., *J. Appl. Cryst.*, **32**, 115—119 (1999).
- 28) DIRDIF94: Beurskens P. T., Admiral G., Beurkens G., Bosman W. P., de Gelder R., Israel R., Smits J. M. M., “The DIRDIF94 Program System, Technical Report of the Crystallography Laboratory,” University of Nijmegen, The Netherlands, 1994.
- 29) Cromer D. T., Waber J. T., “International Tables for X-ray Crystallography,” Vol. IV, The Kynoch Press, Birmingham, 1974, pp. 72—98.
- 30) Creagh D. C., Hubbell J. H., “International Table for X-ray Crystallography,” Vol. C, ed. by Wilson A. J. C., Kluwer Academic Publishers, Boston, 1992, pp. 200—206.
- 31) teXsan: Crystal Structure Analysis Package, Molecular Structure Corporation 1985 and 1999.
- 32) Cysteine was recovered quantitatively as HCl salt under the same conditions without the use of **8e**.
- 33) “The Merck Index,” 10th ed., ed. by Windholz M., Merck & Co., Inc., Rahway, 1983, p. 400.